

# Dynamic Optimization of Vehicle Planetary Transmission Based on GA and FEA

Changle Xiang, Cheng Wang, Hui Liu and Zhongchang Cai

**Abstract** Based on the nonlinear model of vehicle planetary transmission, the dynamic optimization model is established. This work use a combined objective function, internal and external load sharing coefficients and peak-to-peak mesh forces of second stage planetary are taken as objectives. The structure parameters of transmission shafts are considered as design variables. Finite Element Analysis (FEA) is carried out to obtain the bending and torsional stiffness, and the maximal Von-Mises stress constraint. Innovatively, we propose and introduce the nonlinear characteristic constraint aim at increasing the reliability of optimization. The Isight-Matlab-Ansys co-simulation method is applied to build the optimization platform. Finally, the optimization moel of vehicle planetary transmission is solved by Genetic Algorithm (GA).

**Keywords** Dynamic optimization · Nonlinear · Planetary transmission · Genetic algorithm · Chaos

---

F2012-J02-007

---

C. Xiang · C. Wang (✉) · H. Liu · Z. Cai  
School of Mechanical Engineering, Beijing Institute of Technology, Beijing, China  
e-mail: zhiaichengzi@yahoo.com.cn

C. Xiang · C. Wang · H. Liu · Z. Cai  
Science and Technology on Vehicle Transmission Laboratory,  
Beijing Institute of Technology, Beijing, China

## 1 Introduction

With the rapid development of high-speed and heavy-load vehicle transmission, the traditional static design method could not meet the design requirements of transmission, therefore, dynamic optimal design methodology is more and more prevalence.

1986, Houser [1] stated that the next step for the optimization design of gear should introduce the dynamic characteristics. In 1988, Japanese scholar Umezawa [2] provided a curve of helical gear vibration characteristics in order to design low vibration and low noise gears. In 1992, Cai [3] analyzed the static optimization of nonlinear dynamic model. The same year, Wang [4] took the dynamic performance of gear pair as objective, after optimization the dynamic load and the vibration was much smaller than the initial design in a wide range of speeds. Fonseca [5] used genetic algorithms to optimize the static transmission error, which is one of the earliest literatures that introduced genetic algorithm into the gear optimization. LUO [6] used the method of gray relation to change multi-objective optimization to a single objective optimization. Li [7] considered the bearing capacity, volume and stability of operation as objectives, then optimized the gear transmission with self adaptive genetic algorithm. Padmanabhan [8] considered the power, efficiency, volume, center distance as objectives, and then he used genetic algorithms to optimize the gear pair. Finally, the finite element analysis (FEA) was used to carry on further study of tooth bending stress. Recently, Faggioni [9] presented a global optimization method focused on gear vibration reduction by means of profile modifications. The optimization method considered different regimes and torque levels. He also pointed out that the static optimal design of the gear transmission system probability made the dynamic performance of gear transmission even worse. But the nonlinear dynamic characteristic and the bending-torsional coupled stress of shaft was not considered in previous studies.

This paper proposed a nonlinear model of vehicle planetary transmission. Based on the dynamic performance of transmission, the dynamic optimization model was built. This paper introduced the nonlinear characteristic constraint and the bending-torsional coupled Von-mises stress as constraint, innovatively. Then, the co-simulation method is used to build optimization platform. Finally, the dynamic optimization model is solved by genetic algorithm.

## 2 Nonlinear Model of Vehicle Planetary Transmission

Physical model of vehicle planetary transmission (Fig. 1).

There are two forward gears and one reverse gear in this vehicle transmission. The two forward gears correspond to the first and third clutch engagement, while the reverse gear corresponding to the second clutch engagement. In this paper,

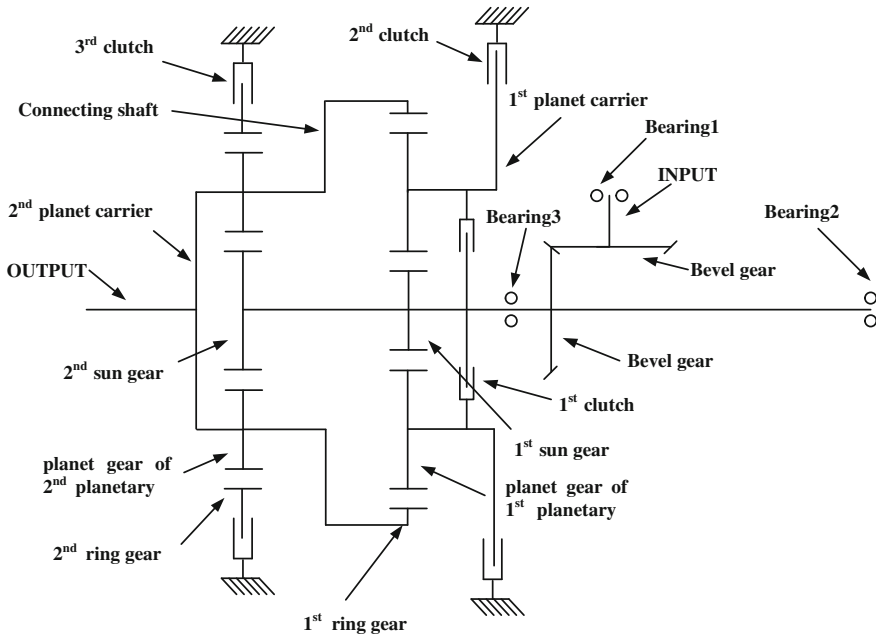


Fig. 1 Physical model of vehicle transmission

we only consider the dynamic performance of first gear. As the engagement of the third clutch, the second planetary is under load while the other with no-load.

Nonlinear dynamic behavior of planetary transmission takes the backlash, time-varying mesh stiffness, installation error and tooth error into consideration [10–12]. The time-varying mesh stiffness is periodic and is expanded in Fourier series form with the gear meshing frequency  $\omega$ , in order to assure the accuracy,  $M = 9$  (Eq. (1)).

$$k(t) = k(t + 2\pi/\omega) = k_0 + \sum_{r=1}^M k_r \cos(r\omega t + \phi_r) \quad (1)$$

Equations (2)–(5) are the nonlinear equations of planetary, where,  $i = 1, 2$ ,  $N = 4$ ,  $j = 1, 2, 3, 4$ . In the equations,  $J$  are moment of inertias,  $R$  are pitch diameters,  $e_M$  are eccentric distances,  $\omega$  are rotational speeds,  $m$  are masses,  $x$  and  $y$  are bending displacements,  $\theta$  are torsional displacements,  $\gamma$  and  $\psi$  are initial phase angles.  $\alpha$  is pressure angle. The index  $s, r, c$  represent the sun, ring, carrier, planet. The index  $i$  and  $j$  represent the stage of planetary, the number of planet gear. The index  $x, y$  represent the direction of bending displacement.

The equations of motion for the sun gears are

$$\begin{aligned}
m_{si}\ddot{x}_{si} - m_{si}e_{Msi}\omega_{si}^2 \cos(\omega_{si}t + \gamma_{si}) + \sum_{j=1}^N \sin(\psi_{pij} + \alpha) F_{sipij} + F_{xsi}^c + F_{xsi}^k &= 0 \\
m_{si}\ddot{y}_{si} - m_{si}e_{Msi}\omega_{si}^2 \sin(\omega_{si}t + \gamma_{si}) - \sum_{j=1}^N \cos(\psi_{pij} + \alpha) F_{sipij} + F_{ysi}^c + F_{ysi}^k &= 0 \\
J_{si}\ddot{\theta}_{si} + \sum_{j=1}^N R_{si}F_{sipij} + T_{si}^c + T_{si}^k &= 0
\end{aligned} \tag{2}$$

where,  $F^c$  and  $F^k$  are damping force and bending forces of sun gear,  $T^c$  and  $T^k$  are relative torques and damping forces between nearby lumped masses.  $F_{sipij}$  is external mesh forces,  $F_{ripij}$  is internal mesh forces.

The equations of motion for the carrier are

$$\begin{aligned}
m_{ci}\ddot{x}_{ci} - m_{ci}e_{Mci}\omega_{ci}^2 \cos(\omega_{ci}t + \gamma_{ci}) - \sum_{j=1}^4 \sin(\psi_{pij} + \alpha) F_{xpij} + \sum_{j=1}^4 \sin(\psi_{pij} - \alpha) F_{ypij} \\
+ F_{xci} + F_{xcir1} &= 0 \\
m_{ci}\ddot{y}_{ci} - m_{ci}e_{Mci}\omega_{ci}^2 \sin(\omega_{ci}t + \gamma_{ci}) + \sum_{j=1}^N \cos(\psi_{pij} + \alpha) F_{xpij} - \sum_{j=1}^N \cos(\psi_{pij} - \alpha) F_{ypij} \\
+ F_{yci} + F_{yc2r1} &= 0 \\
J_{ci}\ddot{\theta}_{ci} - R_{ci} \sum_{j=1}^N F_{ypij} + T_{c2rj} + T_o &= 0
\end{aligned} \tag{3}$$

where,  $F_{xcirj}$ ,  $F_{ycirj}$  and  $T_{cirj}$  are interaction forces of 2nd carrier and 1st ring.  $F_{xci}$  and  $F_{yci}$  are bearing forces,  $T_o$  is block torque.  $F_{xpij}$  and  $F_{ypij}$  are bearing forces of planet.

The equations of motion for the ring gears are

$$\begin{aligned}
m_{ri}\ddot{x}_{ri} - m_{ri}e_{Mri}\omega_{ri}^2 \cos(\omega_{ri}t + \gamma_{ri}) - \sum_{j=1}^N \sin(\psi_{pij} - \alpha) F_{ripij} + F_{xri} &= 0 \\
m_{ri}\ddot{y}_{ri} - m_{ri}e_{Mri}\omega_{ri}^2 \sin(\omega_{ri}t + \gamma_{ri}) + \sum_{j=1}^N \cos(\psi_{pij} - \alpha) F_{ripij} + F_{yri} &= 0 \\
J_{ri}\ddot{\theta}_{ri} - R_{ri} \sum_{j=1}^N F_{ripij} + T_b &= 0
\end{aligned} \tag{4}$$

where,  $F_{xri}$  and  $F_{yri}$  are bearing forces of x, y direction,  $T_b$  is brake torque.

The equations of motion for the planet gear  $j$  are

$$\begin{aligned}
& m_{p_{ij}}\ddot{x}_{ci} \cos \psi_{p_{ij}} + m_{p_{ij}}\ddot{y}_{ci} \sin \psi_{p_{ij}} + m_{p_{ij}}\dot{x}_{p_{ij}} + m_{p_{ij}}(-2\omega_{ci}\dot{y}_{p_{ij}} - \omega_{ci}^2 x_{p_{ij}}) \\
& - m_{p_{ij}}e_{M_{p_{ij}}}\omega_{p_{ij}}^2 \cos(\psi_{p_{ij}} - \omega_{p_{ij}}t - \gamma_{p_{ij}}) - \sin \alpha F_{s_{ip_{ij}}} - \sin \alpha F_{r_{ip_{ij}}} + F_{x_{p_{ij}}} = 0 \\
& - m_{p_{ij}}\ddot{x}_{ci} \sin \psi_{p_{ij}} + m_{p_{ij}}\ddot{y}_{ci} \cos \psi_{p_{ij}} + m_{p_{ij}}\dot{y}_{p_{ij}} + m_{p_{ij}}(2\omega_{ci}\dot{x}_{p_{ij}} - \omega_{ci}^2 y_{p_{ij}}) \quad (5) \\
& + m_{p_{ij}}e_{M_{p_{ij}}}\omega_{p_{ij}}^2 \sin(\psi_{p_{ij}} - \omega_{p_{ij}}t - \gamma_{p_{ij}}) + \cos \alpha F_{s_{ip_{ij}}} - \cos \alpha F_{r_{ip_{ij}}} + F_{y_{p_{ij}}} = 0 \\
& - J_{p_{ij}}\ddot{\theta}_{ci} + (J_{p_{ij}} + e_{M_{p_{ij}}}^2 m_{p_{ij}})\ddot{\theta}_{p_{ij}} - R_{p_{ij}}F_{s_{ip_{ij}}} + R_{p_{ij}}F_{r_{ip_{ij}}} = 0
\end{aligned}$$

For these planet gears, the inertia forces are much more complicated than the other parts due to the planet gears are attached to the carrier. The equations of other lumped mass model are not present here.

### 3 Optimization Model

This section describes about the objective functions, design variables and constraints of dynamic optimization model.

#### 3.1 Objective Functions

The effect of dynamic performance caused by first stage planetary not play a crucial role for the second gear, so we take the internal and external load sharing coefficients and the peak-to-peak meshing forces of second stage planetary as objectives. The objectives are as follows.

$$\begin{aligned}
f_1 &= \frac{\max((F_{r_{2p21}}^m), (F_{r_{2p22}}^m), (F_{r_{2p23}}^m), (F_{r_{2p24}}^m))}{(\sum_{j=1}^4 (F_{r_{2p2j}}^m))/4} \\
f_2 &= \frac{\max((F_{s_{2p21}}^m), (F_{s_{2p22}}^m), (F_{s_{2p23}}^m), (F_{s_{2p24}}^m))}{(\sum_{j=1}^4 (F_{s_{2p2j}}^m))/4}
\end{aligned}$$

where,  $F_{r_{2p2j}}^m$  are the mean internal mesh forces of second stage planetary, respectively.  $F_{s_{2p2j}}^m$  are the mean external mesh forces of second stage planetary, respectively.

$$f_{j+2} = F_{r_{2p2j}}^{p-p}, f_{j+6} = F_{s_{2p2j}}^{p-p}$$

where,  $j = 1, 2, 3, 4$ , represent the external peak-to-peak mesh forces of second stage planetary.

$$\mathbf{f} = [f_1, f_2, f_3, f_4, f_5, f_6, f_7, f_8, f_9, f_{10}]^T$$

There are ten different objectives considered in this work. These objectives can be classified into two groups,  $f_1$  and  $f_2$  are load sharing coefficients,  $f_3$  to  $f_{10}$  are peak-to-peak mesh forces. Since the parameters of each group are on different scales, these factors are to be normalized to the same scale [13]. The normalized objective function is obtained as follows:

$$\text{COF} = \sum_{k=1}^{10} W_k * N(f_k) * N(f_k) = \frac{f_k}{S_k}$$

where, COF is combined objective function.  $N(f_k)$  represent normalized objective.  $W_k$  represent weight factor, all equal to 0.1.  $S_k$  represent normalization factor, for load sharing coefficient  $S_k = 1$ , for peak-to-peak mesh forces  $S_k = 10,000$ .

### 3.2 Design Variables

According to the engineering design requirements, the inner diameters of shaft, the gear parameters and layout of planetary are determined. So there are nine parameters can be taken as design variables, the five outer diameters of shaft,  $R_i$ ,  $i = 1, 2, 3, 4, 5$ , and the layout of bearing 1, 3 and bevel gear  $L_j$ ,  $j = 1, 2, 3$ . The optimization model contains eight independent design variables.

$$\mathbf{X} = [x_1, x_2, x_3, x_4, x_5, x_6, x_7, x_8]^T = [R_1, R_2, R_3, R_4, R_5, L_1, L_2, L_3]^T.$$

### 3.3 Design Constraints

Basically, there are three types of constraints: the boundary constraints, the static performance constraints and the dynamic performance constraints. In order to increase the reliability of optimization result, the nonlinear characteristic constraint is proposed in this work.

#### 3.3.1 Boundary Constraints

Boundary constraints, mainly refer to the lower bound (LB) and the upper bound (UB) of the design variables.

According to the actual parameters variation ranges, the boundary constraints are show in Table 1.

**Table 1** Boundary constraints (unit mm)

	R <sub>1</sub>	R <sub>2</sub>	R <sub>3</sub>	R <sub>4</sub>	R <sub>5</sub>	L <sub>1</sub>	L <sub>2</sub>	L <sub>3</sub>
LB	22	22	22	17	17	100	44.5	148
Initial	27.5	31.5	31.5	22.6	22.6	211.5	44.5	148
UB	35	35	35	22.6	22.6	211.5	156	259.5

### 3.3.2 Static Constraints

The tooth breakage and surface failures are the most likely failures of transmission gears. To safeguard the tooth against the breakage and surface failure, the gear should have adequate bending strength and contact strength. The bending fatigue stresses and crushing fatigue stresses of external meshing are considered.

$$\sigma_F \leq [\sigma_F] \quad \sigma_H \leq [\sigma_H]$$

The bending stress ( $\sigma_F$ ) and contact stress ( $\sigma_H$ ) are adopted from [14]

$$\sigma_F = \frac{F_t}{b m_n} Y_{Fa} Y_{Sa} Y_\epsilon Y_\beta K_A K_v K_{F\beta} K_{F\alpha}$$

$$\sigma_H = Z_E Z_H Z_\beta Z_\alpha \sqrt{K_A K_v K_{H\beta} K_{H\alpha} F_t \frac{1}{d_1 b} \frac{u + 1}{u}}$$

where,  $F_t$  is transmitted tangential load at operating pitch diameter,  $b$  is contacting face width,  $d_1$  is pinion pitch diameter,  $u$  is gear teeth/pinion teeth,  $m_n$  is normal module. The other parameters are mostly correction factors.

The allowable value of bending stress [ $\sigma_F$ ] and contact stress [ $\sigma_H$ ] are 525 and 1650 MPa, respectively.

### 3.3.3 Dynamic Constraints

Bearing is one of the most important parts in vehicle transmission. In order to avoid the fatigue failure of the bearing, the bearing forces should be lesser then the allowable value.

$$F_{iMax} \leq [F_i]$$

where,  $F_i$  is maximal bearing force,  $[F_i]$  is allowable value of bearing. The allowable value of three bearings are 59500, 82500 and 58500 N, respectively.

For bending-torsional coupled transmission shaft, the maximum Von-Mises stress should be considered. FEA method is used to model the shaft at different parameters and calculate the dynamic Von-Mises stress at different time steps. Because of the difficulty to determine all the forces acting on the shaft, the displacements of every lumped mass on shaft are extracted as boundary conditions of FEA.

$$\sigma_{\text{Max}} \leq [\sigma]$$

where,  $\sigma_{\text{max}}$  is maximal dynamic stress,  $[\sigma]$  is allowable value equal to 350 MPa.

### 3.3.4 Nonlinear Characteristic Constraint

The nonlinear dynamic model take time-varying mesh stiffness, backlash and tooth errors into consideration, so it's inevitable to appear chaotic motion for some design variables. In order to avoid chaotic motion, we introduce the nonlinear characteristic constraints. Lyapunov exponent provides one of the most useful test for the presence of chaos [15]. As long as the largest lyapunov exponent ( $\text{LE}_{\text{max}}$ ) is greater than 0, the system appears chaotic motion. It is reasonable that the largest lyapunov exponent is taken as nonlinear characteristic constraint. Here, the method of computing the  $\text{LE}_{\text{max}}$  proposed by Benettin is used [16].

$$\text{LE}_{\text{Max}} \leq 0.$$

## 4 Results and Discussion

The nonlinear dynamic equations of vehicle transmission was solved using the fourth order Runge–Kutta method with input torque and speed of vehicle transmission are 2,000 Nm and 7,000 r/min, respectively. The time series data corresponding to the first 5,000 revolutions of the two gears were deliberately excluded from the dynamic analysis to ensure that the analyzed data related to steady-state conditions [17]. Isight-Matlab-Ansys co-simulation is used to build optimization platform. The optimization flow shows in Fig. 2.

Due to non-analytic of objective functions, the traditional gradient-based optimization method is no longer applicable. So we use modern optimization methods—Binary Coded based Genetic Algorithm (GA) with one-point crossover to optimize the system [18]. The values of Genetic Algorithm operators are shown in Table 2. There are 200 individuals participate in iteration. The Isight automatic determines the parameters of design variables. In order to reduced the mapping error of binary encoding and decoding, the size of gene is set as 20.

The optimal result occurs at step 140. The optimum values of objective function and design variables corresponding to the minimum COF value are shown in Tables 3 and 4. From Table 3, we can conclude that the optimal parameter of L2, L3, R1, R2, R5 are remain the same, while the L1, R3, R4 are reduced. Figure 3 shows the finite element model of shaft with initial parameters and optimal parameters.

From Fig. 4, we can obtain that all the objectives of optimal design are lesser then the initial design more or less exceptt the external peak-to-peak meshing



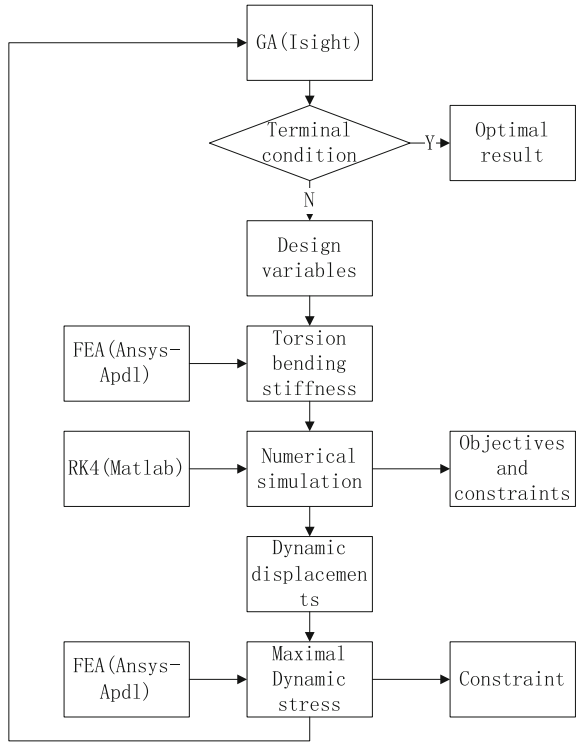


Fig. 2 Optimization flow of co-simulation method

Table 2 Values of genetic operators

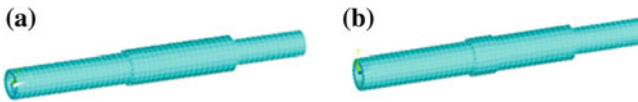
Operators	Values
Gene size	20
Population size	10
Number of generations	20
Crossover rate	1.0
Mutation rate	0.01

Table 3 Parameters of initial and optimal design Unit(mm)

	Initial design	Optimal design
L <sub>1</sub>	211.5	210.74
L <sub>2</sub>	44.5	44.5
L <sub>3</sub>	148	148
R <sub>1</sub>	27.5	27.5
R <sub>2</sub>	31.5	31.5
R <sub>3</sub>	31.5	28.86
R <sub>4</sub>	22.6	22.51
R <sub>5</sub>	22.6	22.6

**Table 4** Objectives of initial and optimal design

	Initial objectives	Optimal objectives	Reduce rates (%)
$f_1$	1.1398	1.1394	0.03
$f_2$	1.1399	1.1395	0.03
$f_3$	24424.695 N	25007.938 N	-2.3879
$f_4$	25544.321 N	24899.610 N	2.5239
$f_5$	25256.015 N	22579.027 N	10.5994
$f_6$	25841.594 N	25097.327 N	2.8801
$f_7$	23842.044 N	23319.950 N	2.1898
$f_8$	25034.291 N	24230.382 N	3.2112
$f_9$	22851.970 N	22145.995 N	3.0893
$f_{10}$	25850.720 N	24472.345 N	5.3321



**Fig. 3** Finite element model of transmission shaft, **a** Initial design. **b** Optimal design

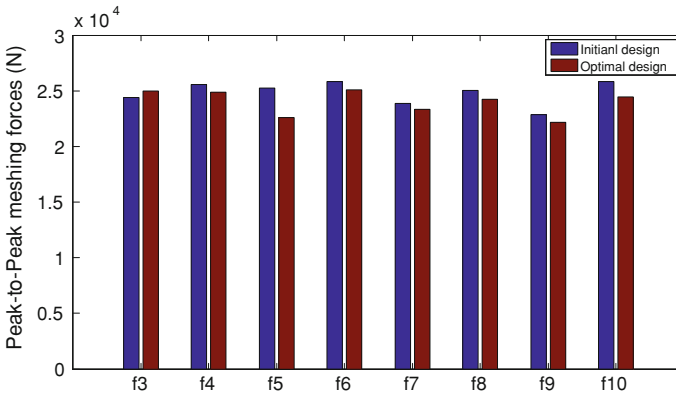


**Fig. 4** Histogram of peak-to-peak mesh forces before and after optimization

forces  $f_3$ , for the sake of naturally conflicting of multi-objective optimization problems (MOP). The reduction rates of peak-to-peak mesh forces shows in the forth column of Table 4. It can be seen that the objective  $f_5$  reduces about 10 %, while  $f_3$  increases about 2 %. The two load sharing coefficients objectives are both less than the initial values about 0.0004, which means that the dynamic characteristic of sharing caused by dynamic load appears to be easing.

Figure 5 shows that as the iteration step goes the design parameters generate by GA seems more and more suitable to satisfy the Von-Mises stress constraint. Dynamic stress analysis was conducted for the transmission shaft before and after design through FEA. Through Fig. 6 we can reach that the Von-mises stress of shaft clearly reduced lower than 300 Mpa at some peaks after optimization. The

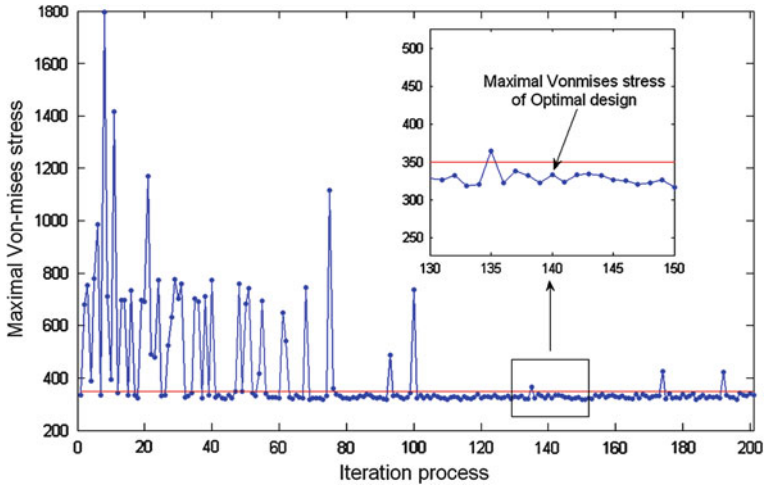


Fig. 5 Maxmal Von-mises stress of shaft

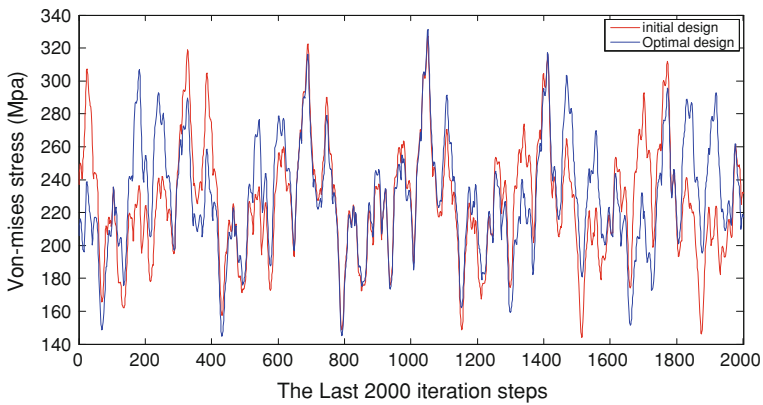


Fig. 6 Dynamic stress of initial and optimal design within the last 2,000 steps

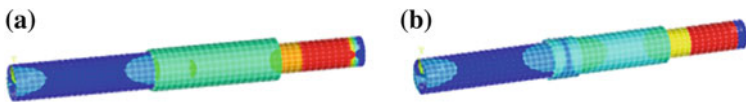
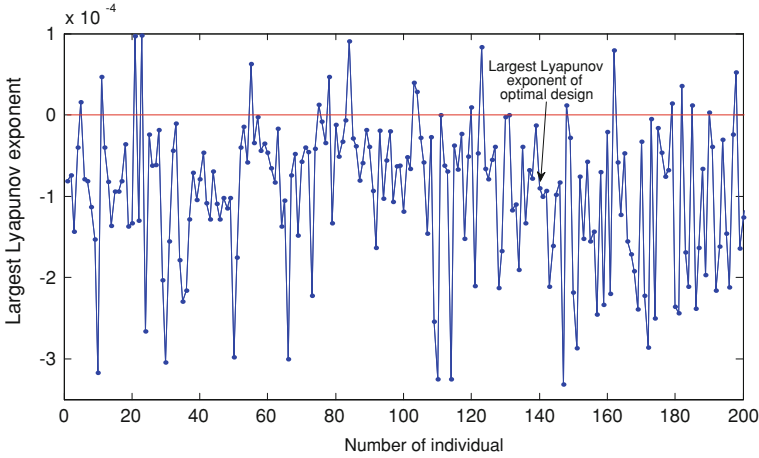


Fig. 7 Von-mises stress of shaft at last calculation step, a Initial design. b Optimal design

maximal Von-mises stress of shaft before and after optimizations are 335 and 333 MPa, which are both less than the allowable value 350 MPa. From Fig. 7, we can realize that the maximal Von-mises stress on the shaft appears between the two sun gears.



**Fig. 8** Largest Lyapunov exponent during optimization

Figure 8 shows there are only 21 group of parameters lead to the chaotic motion of transmission, while the others including the optimal design appear non-chaotic motion. With the nonlinear characteristic constraint, the chaotic solutions have been effectively removed. The largest Lyapunov exponent of transmission under initial design and optimal design are  $-8.1\text{E}-5$  and  $-9.0\text{e}-5$  respectively, which means dynamic motion of initial and optimal design are both non-chaotic.

## 5 Conclusion

A dynamic optimization model, based on the nonlinear dynamic of vehicle planetary transmission, has been built in order to improve the dynamic performance. Parameters of shaft were considered as design variables. In order to improve the reliability of transmission shaft, the finite element method (FEA) is used calculated the maximal dynamic stress constraint. The bending and torsional displacements of lumped masses on shaft were extracted as boundary conditions of FEA. Innovatively, by introducing the nonlinear characteristic constraint, chaos solutions has been effectively removed.

Isight-Matlab-Ansys co-simulation method was used to build the optimization platform. Binary coding Genetic Algorithm was utilized in this work. The optimization model and method proposed in this work are both suitable for the other vehicle transmission.

After optimization, most of the objectives of optimal design were lesser then the initial design more or less. The largest Lyapunov exponent of optimal design transmission was less than zero, which means the dynamic performance of vehicle transmission can predict. The dynamic stress of shaft clearly reduced at some

peaks before and after optimization, but the maximal stress was not significantly reduces. Finally, the optimization results not only avoid the chaotic behaviour, but also improve the dynamic performance of vehicle transmission and extending the system life.

**Acknowledgments** This work was partially supported by Natural Science Foundation of China (50905018,51075033). The authors would like to express gratitude to its financial support.

## References

1. Tavakoli MS, Houser DR (1986) Optimum profile modifications for the minimization of static transmission errors of spur gears. *J Mech Transmissions Autom Des* 108:86–95
2. Umezawa K (1988) Estimation of vibration of power transmission helical gears by means of performance diagrams on vibration. *JSME Int J* 31:598–605
3. Cai Y, Hayashi T (1992) The optimum modification of tooth profile for a pair of spur gears to make its rotational vibration equal to zero. *ASME proceedings of power transmission and gearing conference* (43–2):453–460
4. Wang T (1992) An optimal design for gears with dynamic performance as an objective function. *J Huazhou University* (20–5):13–18
5. Fonseca DJ (2005) A genetic algorithm approach to minimize transmission error of automotive spur gears sets. *Appl Artif Intell* 19–2:53–179
6. Luo Y, Liao D (2009) High dimensional multi-objective grey optimization of planetary gears type AA with hybrid discrete variables. *International conference on computational intelligence and natural computing*
7. Li R, Chang T, Wang J, Wei X (2008) Multi-objective optimization design of gear reducer based on adaptive genetic algorithm. *IEEE* 229–233
8. Padmanabhan S, Ganesan S, Chandrasekaran M (2010) Gear pair design optimization by genetic algorithm and FEA. *IEEE* 301–307
9. Faggioni M (2011) Dynamic optimization of spur gears. *Mech Mach Theo* 46:544–557
10. Guo Y, Parker RG (2010) Dynamic modeling and analysis of a spur planetary gear involving tooth wedging and bearing clearance nonlinearity. *Eur J Mech A/Solids* 29:1022e–1033
11. Kahraman A, Singh R (1991) Interactions between time-varying mesh stiffness and clearance non-linearities in a geared system. *J Sound Vib* 146:135–156
12. Kahraman A, Blankenship GW (1994) Planet mesh phasing in epicyclic gear sets. *International gearing conference Newcastle* 99–104
13. Saravanan R, Sachithanandam M (2001) Genetic algorithm for multivariable surface grinding process optimization using a multi-objective function model. *Int J Adv Manuf Technol* 17:330–338
14. Dudley DW (1983) *Handbook of practical gear design*, McGraw-Hill Book Co, New York
15. Wolf A, Swift JB, Swinney HL, Vastano JA (1985) Determining Lyapunov exponents from a time series. *Physica* 16D:285–331
16. Benettin G, Galgani L, Giorgilli A, Strelcyn J-M (1980) Lyapunov characteristic exponents for smooth dynamical systems and for Hamiltonian systems; a method for computing all of them. *Meccanica* 15:9
17. Cai-Wan Chang-Jian, Chang Shih-Ming (2011) Bifurcation and chaos analysis of spur gear pair with and without nonlinear suspension. *Nonlinear Anal: Real World App* 12:979–989
18. Deb K (2001) *Multi-objective optimization using evolutionary algorithms*. Wiley, Chichester